ce/papers Proceedings in civil engineering

Ernst & Sohn A Wiley Brand

ORIGINAL ARTICLE

eurosteel AMSTERDAM 2023

Ernst & Sohn A Wiley Brand

Experimental Investigation on Buckling Behavior of soil-embedded Piles

Hagen Balscheit[1], Albrecht Victor[2] Marc Thiele[1], Pablo Cuellar[1], Matthias Baeßler[1], Falk Lüddecke[2]

Correspondence

Hagen Balscheit, M.Sc.

Bundesanstalt für Materialforschung und -Prüfung
Fachbereich 7.2 Ingenieurbau
Unter den Eichen 87
12205 Berlin

Email: hagen.balscheit@bam.de

[1] Bundesanstalt für Materialforschung und -Prüfung, Berlin, Germany
[2] Jörss-Blunck-Ordemann GmbH, Hamburg, Germany

Abstract

Monopiles are currently the predominant foundation type for offshore wind turbines in Europe. Due to the increasing dimensions of the turbines, pile diameters beyond 10m become necessary. A design-relevant failure mode of monopiles is the local buckling of the pile wall in the embedded sections. Relevant buckling guidelines do not consider the soil-structure interaction specifically, although the embedment may allow for a reduction of wall thickness. However, Eurocode-based design concepts require a validation with comparative buckling cases for validation, either in terms of buckling curve parameters for both the algebraic stress-based and semi-numerical LBA/MNA design concept or as a calibration factor k_{GMNIA} for fully numerical GMNIA calculations. These parameters are not yet available for embedded shells. To close this gap, we have conducted experiments on piles embedded in sand to investigate local buckling under soil-structure-interaction. The results will be used to calibrate numerical models. This research was carried out as part of the VERBATIM research project, funded by PTJ/BMWK and supported by the Carbon Trust's Offshore Wind Accelerator consortium.

Keywords

Shell Buckling, Monopiles, Soil-Structure-Interaction, Pile buckling, Offshore Foundations

1 Introduction

Monopiles are currently the predominant foundation type for offshore wind turbines in Europe due to the relatively simple manufacturing process, that can be automated to a large extent, as well as the efficient offshore installation procedure. A generic sketch of such a system is outlined in Figure 1. With larger turbines, pile diameters of 10m and beyond and total pile lengths up to more than 60m can become necessary. In this context, any reduction of wall thickness in design leads to significant savings in lifting mass, handling, and production costs. One design-relevant failure mode of the piles is the local buckling of its wall, which may occur in the embedded sections due to the overturning moments induced by the turbine's environmental loading. Due to their geometry, monopiles can generally be considered as shell structures. However, the relevant guidelines on shell buckling do not specifically consider the soil-structure-interaction, although the embedment may allow reductions of the wall thickness.

The Eurocode-based verification procedure specifies either the stress-based design - an algebraic and empirically motivated design concept - or its semi-numerical alternative, the LBA/MNA design. Both concepts describe the buckling limit as a reduction of the plastic load-bearing capacity. The associated reduction factor is defined in terms of a buckling curve. To describe the shape of this curve good knowledge of the governing buckling-curve parameters is required. For typical cylindrical shell structures like chimneys or silos, these buckling curve parameters are provided by annexes of Eurocode 3 Part 1-6 [1]. Further background information is given e.g. in [5] and [12]. The governing formulae are based on empirical data gained by experimental investigations conducted over the past decades. However, the nonlinear nature of the subgrade

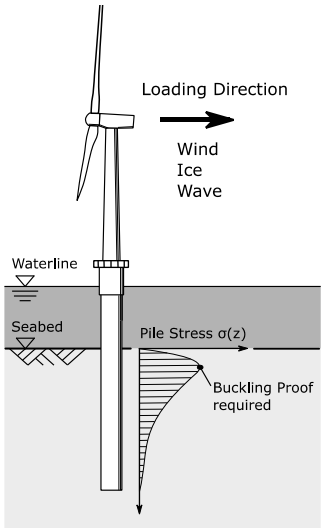

Figure 1 Generic monopile foundation with overturning load direction and qualitative stress distribution

https://doi.org/10.1002/cepa.2313 wileyonlinelibrary.com/journal/cepa

embedment makes an application of the LBA/MNA concept difficult, since it is not obvious a priori at which point the embedment stiffness has to be linearized for the required eigenvalue analysis. Alternatively, design engineers may resort to fully numerical GMNIA computations, where the soil-embedment is often introduced by means of discrete springs distributed over the embedded shell. A systematic experimental validation of such models is still missing thus precluding so far, a derivation of the required numerical calibration factor k_{GMNIA}.

The design standards do not provide a straight-forward approach to consider lateral embedment of shell structures. Most of the existing research on pile stability involving a soil-structure-interaction address only the global column-type buckling, leaving only a few studies actually dealing with the shell buckling phenomenon under lateral embedment. Early works on shell buckling in interaction with another medium were carried out to investigate the buckling resistance of tunnel linings [3]. Other studies have been conducted in the field of aerospace research, aiming at design improvements of solid fuel rockets or on silo structures considering effects of an inner filling (see e.g. the comprehensive literature review provided in [9]). More recent insights can be found in the works of Hübner [9] and Winkel [14]. The former did extensive numerical studies on the buckling behavior of combi wall piles, while the latter presented large-scale field tests on dolphin piles. Some other works have focused on the buckling behavior of suction buckets, see e.g. [6],[8]. These structures have a nonlinear lateral support similar to that of monopiles, but their loading conditions differ significantly, as their buckling limit is triggered by inner suction pressure in contrast to the global bending of monopiles. In addition, the shell slenderness and length differ from that of monopile foundations.

So far, the published data for embedded piles is still very sparse, such that practical design engineers face difficulties in verification and validation of their own models. To address this problem, we conducted a systematic test campaign on piles embedded in sand, where the slenderness of the tested piles matched that of real prototypes and variations in the subgrade stiffness were introduced by pneumatic prestressing of the soil. The buckling tests investigate the governing slenderness and imperfection amplitudes as well as the influence of the inner filling. The actual soil reaction during the tests is reconstructed from pile strain measurements. The new test results will permit the calibration of numerical models allowing design engineers a safer and possibly more economical prediction of the buckling capacity of large monopile foundations.

2 Experimental Setup

The general aim of the setup was the conduction of buckling tests on a variety of embedded piles. The pile embedment was implemented in a large cylindrical vessel of 3m diameter and a height of 2.8m filled with the embedding soil. A special feature of the setup was the ability to vary the stress state (and thus the stiffness) of the soil in a controlled manner by means of airtight hoses wrapped along the inner wall of the soil container. This allowed the application of lateral pressure to the soil body, as already demonstrated in [10]. In the same vein, the top surface of the soil was covered with semi-circular pneumatic pillows and a stiffened lid to allow for application of vertical pressure on the soil body. For load introduction two hydraulic rams have been installed on the surrounding steel frame that allow lateral as well as axial loading at the head of the pile specimen. The used subgrade material is a uniformly graded sand from a pit near Berlin (a comprehensive description of the soil properties is given in [7]). An isometric sketch of the test rig is shown in Figure 2. The dimensions of the model piles were aligned to the slenderness of existing and future offshore prototypes. This resulted in 3m long sample pipes of 200mm diameter and different thicknesses between 1mm and 2mm. The piles were made from a cold rolled steel (DC01 | 1.0330), curved round and welded by the supplier. As the specimen are mainly affected by bending, the influence of the welding seam can be reduced by its alignment on the tensile fiber. Potential geometric stiffening introduced by the seam may be tracked by imperfection assessment.

The geometrical shape of the piles including imperfections, was recorded by means of 3D-scans. This was done before and after each test, utilizing a T-SCAN-hawk handheld scanner fabricated by ZEISS. Some of the tests were devised to include artificial dent imperfections, pressed into the piles, to assess the imperfection sensitivity under nonlinear embedment. Due to the thin wall thickness of the model piles and to avoid the introduction of heavy ovalisation, a two parted wedged plug was manufactured and introduced into the specimen during the denting process. With their wedged surfaces, both plug parts can be clamped against each other allowing its precise alignment along the pile length. The dents can then simply be applied by hammering a round steel bar against the pile surface at the intended position. Figure 3 illustrates the process of dent application exemplary at the head of an old pile specimen from an already completed test.

Numerous strain gauges were applied to the model piles, most of which were uniaxial gauges aligned in an equidistant pattern below the subgrade surface (see Figure 4). This would later permit a reconstruction of the subgrade reaction based on the global bending behavior of the pile. In addition to this, some triaxial rosette gauges were placed directly at the subgrade surface and 500mm above, aligned orthogonal to the loading direction, to allow a reconstruction of the actual introduced transversal loads. The pile displacement is measured with wire displacement transducers at 3 positions above the ground and an additional one at the pile tip. The wire of the tip displacement transducer is guided through a small plastic pipe that ends a few centimeters in front of the tip in order to avoid blockage of the wire due to soil friction. In addition, 120mm-long strain gauges were installed in the region of the expected buckle to trace the development of the buckling process over time. Such gauges are usually used for tests on concrete components and served here only as a qualitative indicator and not for direct strain measurement. During the first two tests also the use of small footprint total orientation sensors of type bno055 was explored. This type of sensor is comparable to the orientation sensors that are used in modern smartphones. It was expected that these 9-DOF sensors would provide useful additional information about the pile deformations in the soil. Unfortunately, the velocity thresholds of these sensors

turned out to be too high to provide meaningful records within the range of the applied loading velocities.

Before installation, the tips of the model piles were closed with an aluminum plate of the same diameter to withstand the introduced axial force. Otherwise, due to insufficient skin friction between pile and soil in this scaled setup, the piles would be simply pushed down to the bottom of the vessel. The piles were installed in a wished in place situation, so that the pile is embedded along half of its length, respectively 1.5m. After levelling and compaction of the bottom subgrade layer, the pile specimen was aligned with the position of the hydraulic cylinders and fixed in place temporarily. Then the sand was installed and compacted layer by layer in depth steps of 20cm. A preliminary approximate calculation indicated the required mass per subgrade layer in order to reach a medium-dense soil compactness. The spatial homogeneity of the soil's relative density was controlled by means of cut-out samples and dynamic probing.

The tests carried out so far have been performed both with and without the use of pneumatic soil prestressing. The vertical load applied at pile head was set to a fixed value of 10kN for all tests, regardless of the slenderness of the shells, since the load from overlying components would remain unchanged by a change in pile thickness for real prototypes. This load magnitude is based on the stress ratios of a D/t =100 pile in combination with the loads of the frequently cited 10MW DTU reference turbine [4]. After application of the axial load, the horizontal hydraulic cylinder was always displaced at a load speed of 0.5mm/s. This speed was chosen such that the loading speed is low enough to exclude dynamic load magnifications, but fast enough to minimize the effects of creep processes in the soil. The tests with pneumatic subgrade prestressing have all been carried out with a lateral pneumatic pressure of about 1bar and a vertical pneumatic pressure of about 2bar. An overview about the tested configurations is given in Table 1.

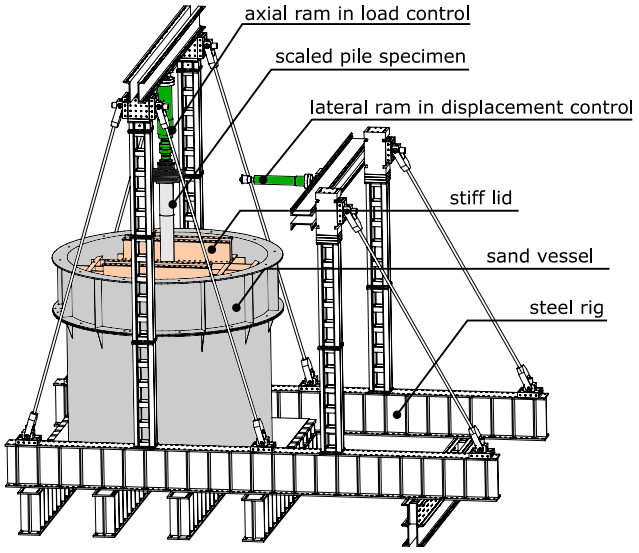

Figure 2 Test setup with installed pile specimen

Table 1 List of test configurations performed so far, where t denotes thickness and $h_{s,i}$ denotes height of inner soil level (see also Figure 4)

Test	t [mm]	imperfect shape	$h_{s,i}$ [mm]	Soil pre-stressing
EP_01	2	as-built	±0	no
EP_02	2	as-built	±0	yes
EP_03	1.5	as-built	±0	yes
EP_04	1.5	as-built	±0	no
EP_05	1	as-built	-50	no
EP_06	1	as-built	+1500	no
EP_07	1	applied dent	±0	yes

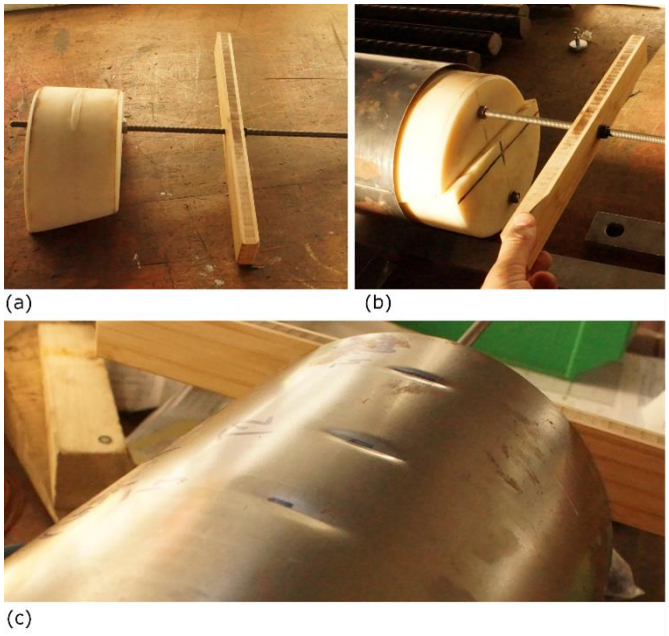

Figure 3 Imperfection application tested on an old sample from an already completed test (a) support wedge with groove, (b) both wedges inserted into the pipe, (c) resulting imperfection patterns

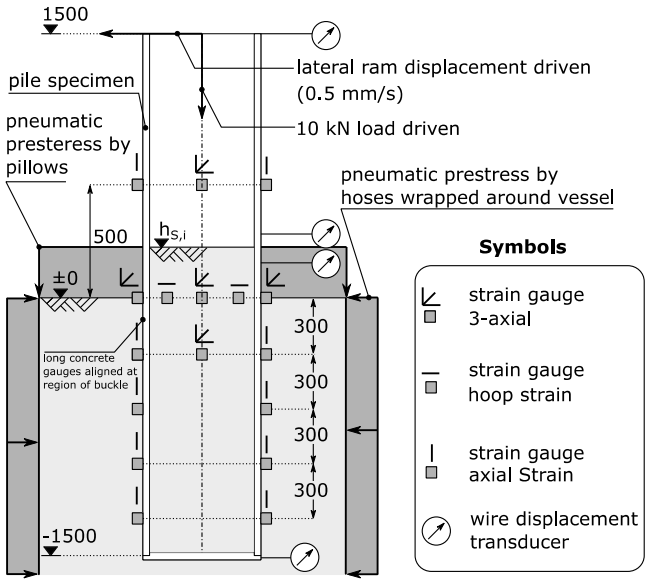

Figure 4 Simplified sketch of the applied instrumentation program

3 Calibration Model

In the numerical analysis of foundation structures, it is important to model the bedding properties realistically. Currently available numerical software in combination with powerful computers, allow a mechanical analysis of embedded piles in a realistic continuum model. For caisson foundations, stability analyses are currently also performed with such models (e.g. [15]). This is possible, as the driving suction triggers large buckling modes that are distributed over the hole shell surface, allowing for a relatively coarse finite element mesh. For buckling analysis of embedded piles however, such models still involve an unreasonable amount of numerical cost. This is mainly since the buckling modes of embedded piles under bending only occur very locally in a small region of the pile surface, which leads to the requirement of a very small element size in relation to the overall model dimensions, to be able to resolve the smallest possible buckling mode. A more robust but simplified approach uses nonlinear springs to replace the subgrade continuum. From a practical design engineers' perspective, it is very convenient to derive the associated spring characteristics from so-called p-y-curves, since various formulations of them are readily available for many relevant soil conditions. These curves describe the lateral pile behavior below the soil surface literally as displacements y versus activated soil reactions p. A widely-used formulation is provided by the API [2] and goes back to studies by Reese and Cox conducted in the 1970s [11]. More modern formulations considering the large dimensions of current monopiles have been proposed in the frame of the PISA-Project [13]. Since the classic p-y-curves describes the pile only as a one-dimensional system in the sense of a Winkler approach, an investigation of shell models in the 3D space requires an adaption to distribute the embedment stiffness properly around the shell model. Another way to define these modified p-y-curves, is by preliminary analysis of a continuum model for assessment of nodal displacements and contact forces. In any case, the buckling model contains nonlinear springs that are distributed around the embedded surface. Similar definitions can also be introduced for the case of a longitudinal soil resistance (the so-called t-z curves), which is out of the scope of this study.

The p-y curves for the calibration model are based on the subgrade reaction activated in the lab test. To determine this, the mobilized subgrade reaction and deformation is derived for each test based on the measured discrete displacements and strains. This inverse problem is solved numerically using a simple beam model in which the soil stiffness per load step is defined by a parametric function. The corresponding stiffness function parameters are then iteratively varied until the error in strain and displacement with respect to its measured magnitudes is minimized. The calibration model used for back-calculation of the performed buckling tests does only consider the effect of lateral springs. Skin friction is considered negligible in the setup due to the vertical displacement constraint, that is created by the pile's baseplate. The cylindrical shell model contains rigidly connected remote nodes on both bottom and top edge. The bottom remote node is fixed in all translational degrees of freedom to account for the effect of the baseplate. The top remote node is used for load introduction. The p-y curves reconstructed from the test records are considered in form of nonlinear springs aligned along the embedded surface. A generic sketch of this FE-Model is outlined in Figure 5.

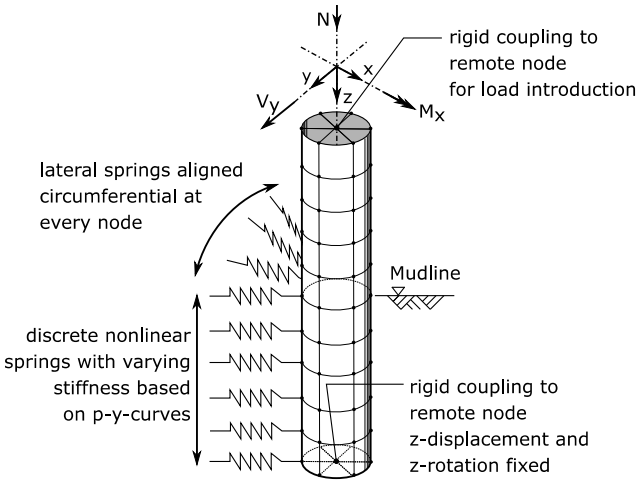

Figure 5 Principle sketch of the numerical model which is to be calibrated based on the test results

4 Selected Results

Even though the test series is not yet completed, we can already present some selected results. As described before the activated subgrade reactions to be used as a boundary condition in the calibration model can be derived from the recorded strains and displacement. Figure 6 presents an exemplary resulting load-displacement relationship for the tested scenario EP-07. The two panes display respectively the longitudinal profiles of mobilized subgrade reaction and the corresponding lateral pile displacement, which is applied as a boundary condition to the numerical model in form of nonlinear springs. As indicated by the color legend, curves of same color belong to the same load step.

Figure 7 shows a plot of the lateral pile-head displacement against the lateral force at the pile head for all conducted tests. There the influence of the wall thickness on the buckling load can be clearly seen. Interestingly, the applied soil prestressing has not an obvious influence on the maximum loads achieved in the test. However, it can be clearly seen that the failure state is reached at larger lateral displacements in the absence of pneumatic prestress. In addition, the test observations indicate that the buckling location and the collapse mode are dependent on the lateral stiffness ratios of soil and steel structure.

With the reconstructed soil reaction, a back-calculation of the test can be performed. Figure 8 shows a resulting lateral load-displacement chart at the pile head comparing FEM-prediction and test result. The test was conducted with a pre-dented pile of 1mm wall thickness and activated pneumatic pressure. Test record and numerical prediction agree well in the initial loading phase as well as during unloading after the buckling event has already occurred. However, in the range where the instability occurs, there is still a comparatively strong overestimation of the buckling load by the model. Nevertheless, a comparison of the post buckling displacement between test and numerical model as it is exemplary displayed in Figure 9 shows good agreement.

5 Discussion and Outlook

As mentioned before, an application of the algebraic stress-based proof and its descendent, the LBA/MNA concept renders difficulties for practical design engineers. On one hand, both concepts rely on a proper determination of the ideal buckling stress respectively the linear buckling eigenvalue. On the other hand, load reduction driven by imperfections of the real structure is empirically based on non-embedded cylindrical shells. However, the nonlinear boundary condition imposed by the soil embedment precludes a preliminary estimation of the point of operation at which the structure would buckle and at which the linear buckling analysis would have to be performed. This forces the analyst to extend the analysis to more complex models using the GMNIA concept.

A plausibility check and verification of the numerical models generated in this way is still difficult due to the scarcity of available validation data. In this sense the current study provides a valuable database for model calibration. In the tests carried out so far on specimens that have not been pre-dented, good agreement between test data and numerical back-calculation was achieved. The result regarding the artificially created imperfection which is presented here still raises questions.

In any case, the presented test results show good agreement with the numerical prediction both in the first loading phase and in the unloading phase after buckling. It can be demonstrated that the essential stiffness conditions prevailing in the test setup are well reproduced by the model. Although the deviation of peak loads (<15%) may create doubts on the predicted buckling limit of the numerical model, it is precisely this deviation that hides the questions of interest in the context of this research. The possible causes can be numerous. To name a few, these include the influence of mesh size, of residual stress, of local plate thickness imperfections, scattering of the Young's modulus, insufficient consideration of spatial embedment stresses etc.. The causes of these deviations are analyzed in greater depth. In this sense, additional back-calculations will be performed using a continuum model for the soil to capture better the influence of the spatial bedding distribution on the buckling behavior. Overall, the test results represent a very valuable database for further model validation.

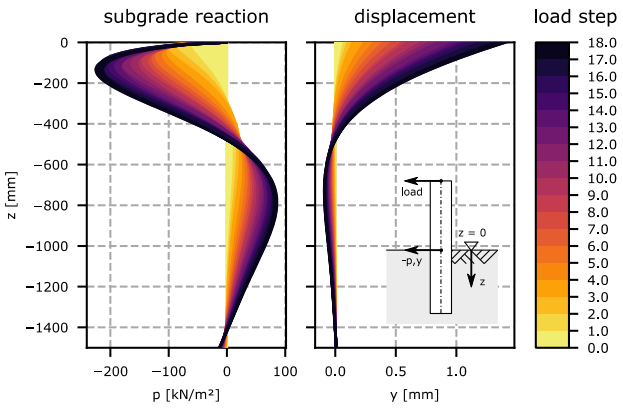

Figure 6 Mobilized subgrade reaction p vs. lateral displacement y based on Test EP-07 with additionally applied pneumatic prestress of soil body

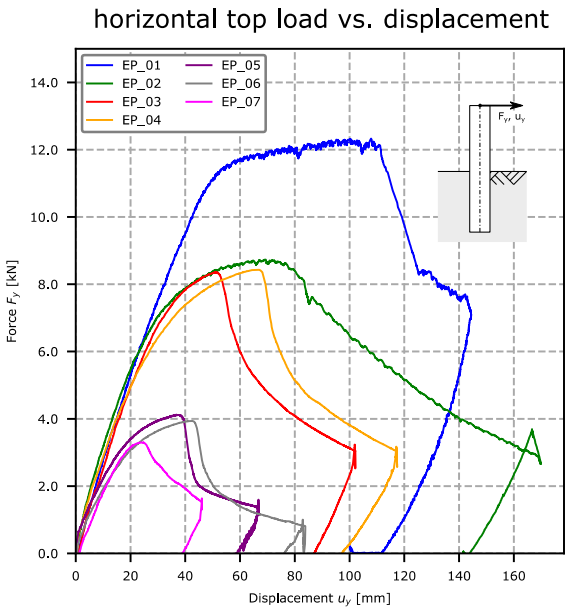

Figure 7 Lateral load-deflection curves over all conducted tests.

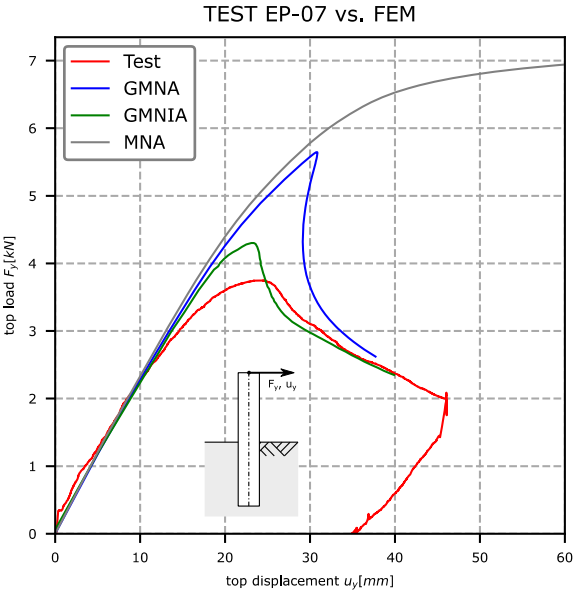

Figure 8 Comparison of prediction and test result for lateral load deflection behavior at pile head for tested scenario EP-07

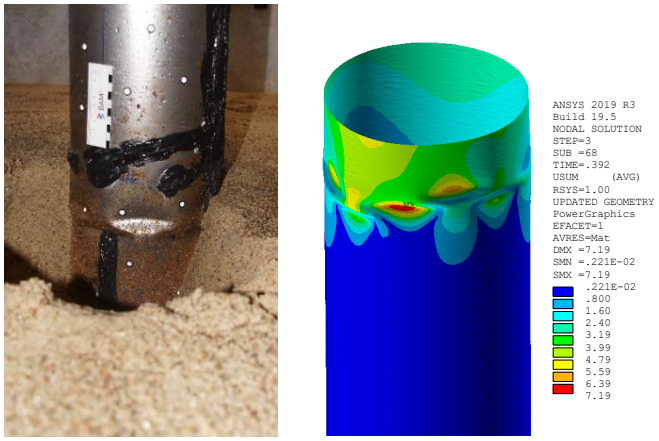

Figure 9 Left: Observed Post buckling displacement; Right: FEM predicted post buckling displacement. The color band indicates the magnitude of lateral displacement (in direction of radial axis), Elements above ground are hidden

Acknowledgements

The material presented here was developed within the VERBATIM research project, funded by PTJ/BMWK and supported by the Carbon Trust's Offshore Wind Accelerator consortium.

The authors would also like to thank the team at the Steel Construction and Mixed Building Technology Unit at the University of Innsbruck, headed by Prof. Lang. Our many interesting discussions have always provided interesting perspectives and supported the successful completion of our work.

References

[1] DIN EN 1993-1-6:2017-07. (2017) *Eurocode 3 - Design of steel structures- Part 1-6: Strength and Stability of Shell Structures*

[2] API RP 2A-WSD. (2002) *Recommended Practice for Planning, Designing and Constructing Fixed Offshore Platforms – Working Stress Design*, API, Edition 21

[3] Amstutz, E. (1950) *Das Einbeulen von Schacht- und Stollenpanzerungen.* Schweizerische Bauzeitung 68, H 9, pp. 102–105

[4] Bak, C.; Zahle, F. (2015) *The DTU 10MW Reference Wind Turbine*, Presentation at Science Meets Industry, Bergen, DTU Wind Energy.

[5] Rotter, J.M.; Schmidt, H. (Eds.) (2013) *Buckling of Steel Shells European Design Recommendations; 5th Edition Revised Second Impression*. ECCS- European Convention for Constructional Steelwork

[6] Foglia, A.; Quiroz, T.; et Al. (2022) *Aktuelle Untersuchungen an Suction Buckets für Offshore-Windenergieanlagen – das ProBucket-Projekt*. Bautechnik 99, Issue 9, pp. 669-678

[7] Georgi, S. (2014) *Experimentelle Untersuchungen zu Verformungsakkumulationen und Tragfähigkeitsreduktion zyklisch belasteter Pfahlgründungen*, PhD Thesis, TU-Berlin

[8] Gottschalk, M. (2016) *Zur Beultragfähigkeit von Suction Buckets.* PhD Thesis, Schriftenreihe des Instituts für Stahlbau, H 33, Universität Hannover, Germany.

[9] Hübner, A. (2007) *Tubular Piles – Buckling in a Complex Situation*, PhD Thesis, Universität Fridericania zu Karlsruhe (TH)

[10] Hübner, A; Saal, H; Charue N, Holeyman A; et Al. (2009) *Enhanced Economy of Tubular Piles by Improved Buckling Design, Final Project Report,* Research Fund for Coal and Steel of the European Commission

[11] Reese, L C; Cox, W. R.; Koop, F. D. (1974) *Analysis of laterally loaded piles in sand* in: Offshore Technology Conference. Pp. 473-483 Houston TX: One Petro

[12] Schmidt, H. (2000) *Stability of steel shell structures*, Journal of Constructional Steel Research 55, H 1, pp. 159–181, Elsevier

[13] Harvey J. Burd, David M. G. Taborda, et Al. (2020) *PISA design model for monopiles for offshore wind turbines: application to a marine sand*; Géotechnique 70 Issue 11, pp. 1048-1066

[14] Winkel, J. (2016). *Large diameter dolphin piles- The effect of the inner soil on their local buckling resistance*, M.Sc. Thesis TU Delft.

[15] Lampert, R; Eckardt, S; Schlegel, R; Rognlien, K; Halvorsen, F. (2018) *Nonlinear 3D FE-Stability analysis of suction pile*, EAGE Annual Conference 2018, European Association of Geoscientists and Engineers: Copenhagen 2018